Polyhedron 45 (2012) 229–237

Contents lists available at SciVerse ScienceDirect

Polyhedron

journal homepage: www.elsevier.com/locate/poly

Nucleophically transformed N-heterocyclic nitriles trapped by cyanooxomolybdates(IV): Crystallographic and spectroscopic study

Anna Ryniewicz, Monika Tomecka, Janusz Szklarzewicz *, Dariusz Matoga, Wojciech Nitek

Faculty of Chemistry, Jagiellonian University, Ingardena 3, 30-060 Kraków, Poland

ARTICLE INFO

Article history:
Received 27 March 2012
Accepted 7 July 2012
Available online 20 July 2012

Keywords:
Molybdenum(IV)
2,3-Dicyanopyrazine
2-Pyridinecarbonitrile
Nitrile reactivity
Crystal structure

ABSTRACT

The reaction of $K_3Na[Mo(CN)_4O_2]\cdot 6H_2O$ with 2,3-dicyanopyrazine or 2-pyridinecarbonitrile in aqueous media results in isolation of two new compounds of formulae $(PPh_4)_2[Mo(CN)_3O(pzac)]\cdot 2H_2O$ (Hpzac = 3-carbamoyl-2-pyrazinecarboxylic acid) and $(PPh_4)_2[Mo(CN)_3O(pynccn)]\cdot 3H_2O\cdot EtOH$ (Hpynccn = 2-pyridineiminocarbonitrile) respectively. X-ray single crystal structure measurements as well as physicochemical measurements confirm transformations of 2,3-dicyanopyrazine to 3-carbamoyl-2-pyrazinecarboxylic acid and 2-pyridinecarbonitrile to 2-pyridineiminocarbonitrile. All complexes are characterized by elemental analysis, IR and UV–Vis spectroscopy. Metal-assisted ligand transformations are studied spectrophotometrically in the pH range 8.5–11.5. Two different pathways of nitrile reactivity are shown and discussed.

1. Introduction

Aromatic nitriles such as 2,3-dicyanopyrazine and its derivatives have been found to be very important not only due to their reactivity but also their possible applications as OLED components [1], in supramolecular chemistry, and as spacer ligands in the formation of metal-organic frameworks (MOFs) [1–3]. They are very strong electron acceptors and thus can be applied as second-order nonlinear optics materials [2,4]. Derivatives of 2,3-dicyanocarbonitrile have also been found to be biologically active, for example they exhibit antibrochospastic activity [5], inhibit the activity of p38 MAP kinase [6], cyclin-dependent kinases and show antiproliferative activity [7]. Due to the presence of chromophore groups, they have been used for the preparation of azaphthalocyanines and applied in photodynamic therapy, non-linear optics, as dyes etc. [8,9]. The properties of cyano derivatives can be easily modified by their coordination to a metal center [10].

On the other hand it is well known that nitriles undergo hydrolysis to carboxylic acids both in acidic and basic solutions and that this process is accelerated even by six orders of magnitude in the presence of d-electron metals. Thus it is very important to understand the role of metal in this process, as well as to understand the influence of metal on electron properties of nitriles demonstrated by their spectra and reactivity. It has been believed that the acceleration of nitrile hydrolysis is induced by the coordination of a nitrile nitrogen to a metal center that changes the electron density on nitrogen and thus affects the hydrolysis [11]. This is probably the only possible mechanism for simple nitriles that do not contain any other donor atoms. However, it is interesting to study more complicated systems, where a competition between donor atoms is possible. It must be stressed, that d-electron metal complexes with nitriles are used also in stabilization of nitriles by their coordination, this is important for example in utilization of nitriles as dyes [10].

In our previous studies on a hydrolysis of 2-cyanopyrazine assisted by the presence of Mo(IV) center [12] it has been found that in aqueous-ethanolic solutions it is possible to isolate, with a high yield, a complex with monodentate 2-cyanopyrazine as a ligand. The ligand is coordinated not *via* the nitrile ligand, but through a heteroaromatic nitrogen atom. It has also been possible to isolate the next transient species with hydrolyzed 2-cyanopyrazine, the 2-pyrazinecarboxylic acid, still coordinated in a monodentate mode with the same nitrogen donor atom. After prolonged reaction time, the most stable complex with bidentate 2-pyrazinecarboxylate bonded through N,O donor atoms has been isolated. All those complexes were characterized by single X-ray crystal structures as well as by elemental analysis, ^1H and ^{13}C NMR, IR and UV–Vis spectra. All these results indicate that the role of a metal is much more complicated than suggested earlier in the literature, and simple coordination of a metal to nitrile nitrogen may be not so important in nitrile hydrolysis. In the presence of the excess of KCN it has also been possible, for the first time in this class of compounds, to introduce a cyanide to an organonitrile group with a formation of an α-iminonitrile coordinated to the molybdenum(IV) atom in a bidentate mode. The resulting complex with the α-iminonitrile has been

* Corresponding author.
E-mail address: szklarze@chemia.uj.edu.pl (J. Szklarzewicz).

0277-5387/$ - see front matter © 2012 Elsevier Ltd. All rights reserved.
http://dx.doi.org/10.1016/j.poly.2012.07.006

isolated and characterized by X-ray single-crystal structure [13]. It has been found that the Mo(IV) center, based on $[Mo(CN)_4O_2]^{4-}$ precursors, is very useful in the study of complexation mechanisms due to both its limited possibility of ligand coordination as well as the ability to indicate a ligand donor atom first coordinated to the Mo center [14]. It also allows insight into whether the complexes isolated are formed on the kinetic or thermodynamic way [15]. This greatly facilitates the study of reaction mechanisms.

In this work we focus on 2,3-dicyanopyrazine and 2-pyridinecarbonitrile alkaline hydrolysis assisted by the presence of $[Mo(CN)_4O(L)]^{n-}$ (where L = OH^- or H_2O, n = 2 or 3) complex ions in aqueous-ethanolic mixtures. The products of the reactions, $[Mo(CN)_3O(pzac)]^{2-}$ or $[Mo(CN)_3O(pynccn)]^{2-}$ ions (where Hpzac = 2,3-pyrazinedicarboxylatomonoamide and Hpynccn = pyridinecyanoimine) are isolated as PPh_4^+ salts and characterized both structurally and physicochemically.

2. Experimental

2.1. Materials and methods

$K_3Na[Mo(CN)_4O_2]\cdot 6H_2O$ was synthesized according to published methods [16]. All other chemicals were of analytical grade (Aldrich) and were used as supplied. Microanalysis of carbon, hydrogen and nitrogen were performed using Elementar Vario MICRO Cube elemental analyzer. Solid samples for IR spectroscopy were compressed as KBr pellets and the IR spectra were recorded on a Bruker EQUINOX 55 FT-IR spectrophotometer. The electronic absorption spectra were recorded with Shimadzu UV-3600 UV–Vis–NIR spectrophotometer equipped with a CPS-240 temperature controller. Diffuse reflectance spectra were measured in $BaSO_4$ pellets with $BaSO_4$ as a reference on Shimadzu 2101PC equipped with an ISR-260 integrating sphere attachment.

The reaction of $K_3Na[Mo(CN)_4O_2]\cdot 6H_2O$ with nitriles (2,3-dicyanopyrazine and 2-pyridinecarbonitrile) was studied in H_2O–EtOH mixture (2:1 v/v) at pH 8.5, 9.5, 10.5 and 11.5 (± 0.1) at T = 313 K. The complex to ligand molar ratio was 1:10 with Mo(IV) concentration equal to $4 \cdot 10^{-3}$ mol/dm^3. The pH was stabilized with a universal buffer [17]. The pH values were measured using Elmetron CP-401 pH meter. The complex was dissolved in the required buffer, thermostated for 5 min and ligand EtOH solutions (also thermostated) of required concentration were added prior to measurements using automatic pipettes with ±0.0001 ml accuracy. The spectra were measured on Shimadzu UV-3600 UV–Vis–NIR spectrophotometer equipped with a CPS-240 temperature controller in 1-cm quartz cuvettes. Since band intensities in the UV part are much higher than in the visible region, the reacting mixtures were transferred to 1-cm cuvettes for measurements in the visible region, and parts of these mixture were diluted 38 times for UV measurements. The spectra were measured interchangeably in both cuvettes.

2.2. Synthesis of $(PPh_4)_2[Mo(CN)_3O(pzac)]\cdot 2H_2O$ (**1**)

$K_3Na[Mo(CN)_4O_2]\cdot 6H_2O$ (1.05 g, 2.19 mmol) was dissolved in water-ethanol mixture (60 ml, 2:1 v/v) and 2,3-dicyanopyrazine (0.28 g, 2.7 mmol) in ethanol (10 ml) was added. The pH of the mixture was lowered from initial 12.7 to 9.2 with 3 M HCl. The dark violet mixture was heated to 50 °C for 30 min and evaporated to dryness. The residue was washed with acetone, dissolved in water with the addition of *ca.* 10% excess of $(PPh_4)Cl$. The resulting dark green solid was filtered off, washed with water and dried in air at room temperature. Yield: 0.10 g (4.3%). *Anal.* Calc. for $C_{57}H_{48}N_6O_6P_2Mo$: C, 63.93; H, 4.52; N, 7.85%. Found: C, 63.19; H, 4.41; N, 7.92%.

2.3. Synthesis of $(PPh_4)_2[Mo(CN)_3O(pynccn)]\cdot 3H_2O\cdot EtOH$ (**2**)

$K_3Na[Mo(CN)_4O_2]\cdot 6H_2O$ (0.50 g, 1.0 mmol) was dissolved in water (25 ml) and 2-pyridinecarbonitrile (0.15 g, 1.4 mmol) in ethanol (5 ml) was added with stirring followed by dropwise addition of 3 M HCl until pH = 11.5 was reached. The resultant dark blue solution was treated with PPh_4Cl (0.40 g, 1.1 mmol). After several days dark green crystals (**2**) were filtered off, washed with water and dried in air at room temperature. Yield: 0.070 g (12%). *Anal.* Calc. for $C_{60}H_{56}MoN_6O_5P_2$ (**1**): C, 65.57; H, 5.14; N, 7.65. Found: C, 65.90; H, 4.83; N, 6.96%.

2.4. Crystallographic data collection and structure refinement

The crystal of **1** suitable for X-ray analysis was isolated from the material prepared as described in Section 2.1. Intensity data were collected on a Nonius Kappa CCD diffractometer using graphite monochromated Mo Kα radiation, λ = 0.71073 Å. The crystal data, details of data collection and structure refinement parameters are summarized in Table 1. The positions of all atoms were determined by direct methods. All non-hydrogen atoms were refined anisotropically using weighted full-matrix least-squares on F^2. Hydrogen atoms H5AA, H5BB, H6AA, H6BB, H6A and H6B were identified on difference Fourier maps and refined with geometrical restrains. All other hydrogen atoms were included in the structure at idealized positions.

The structure was solved using SIR-97 and refined by SHELXL program [18,19].

Single crystals of **2** suitable for X-ray diffraction measurements were obtained from the filtrate in the synthesis described in Section 2.2. The crystal structure of **2** was measured several times on different crystals coming from different synthetic conditions and from recrystallized samples. In all cases the structures refinements led to high R factors (*ca.* 20%) in spite of the fact that there were no problems with crystal quality (such as for example with mosaicity). In all cases the same complex formula and the same anion structure (within experimental error) were found. Since the crystal data were consistent with elemental analysis and spectro-

Table 1
Crystal data and structure refinement parameters for **1**.

	1
Empirical formula	$C_{57}H_{48}MoN_6O_6P_2$
Formula weight	1070.89
Crystal size (mm)	0.40 × 0.25 × 0.05
Crystal system	triclinic
Space group	$P\bar{1}$
a (Å)	8.004(5)
b (Å)	13.432(5)
c (Å)	25.022(5)
α (°)	85.277(5)
β (°)	86.881(5)
γ (°)	77.785(5)
h	−10 to 10
k	−17 to 17
l	−32 to 32
V (Å^3)	2618
Z	2
T (K)	293
D_c (Mg/m^3)	1.358
Reflections measured	36769
Reflections unique	11667
Restrains	657
Reflections observed [$I > 2\sigma(I)$]	9946
R indices [$I > 2\sigma(I)$]	
R	0.0310
wR_2	0.0859
S	1.072

scopic data, we present here the anion structure and we discuss it only roughly as an the indication of iminonitrile formation.

3. Results and discussion

3.1. Crystal structures

The crystal structure of **1** contains $[Mo(CN)_3O(pzac)]^{2-}$ anion, two PPh_4^+ cations and two water molecules. The selected bond lengths and angles are listed in Table 2 whereas the anion structure is presented in Fig. 1. The organic ligand coordinates in a bidentate mode to afford a distorted octahedral geometry with three cyano ligands and nitrogen atom of pzac in equatorial positions as well as oxo ligand and carboxylate oxygen (O_2) occupying axial positions.

The anion is strongly distorted: *e.g.* the O2–Mo1–O1 angle is 164.30° and the angles C–Mo1–O1, O1–Mo1–N4 are 98.90° and 91.97°, respectively. A similar type of deformation is observed for all known up until now Mo(IV) complexes $[Mo(CN)_3O(LL)]^{n-}$ ($n = 1$ or 2) [20]. The average Mo1–C and C≡N bond distances are 2.171 and 1.135 Å, respectively and are very similar to those found in the structure of $[Mo(CN)_3O(pic)]^{2-}$ anion, where the bond lengths are 2.161 and 1.148 Å, respectively [21]. Cyano ligands are not all bound with the same strength, the Mo1–C2 bond is the shortest (2.151 Å), and this bond shortening is probably caused by its *trans* location to the Mo1–N4 bond and therefore the longest bond C2–N2 is observed. This indicates significant $Mo^{IV} \rightarrow CN$ π-back-bonding and the CN^- ligand exerts a relatively large structural trans effect in this complex by competing with the weaker N-donor pyrazine ligand for π-electron density [22]. The coordination of $pzac^-$ ligand to molybdenum center is close to that found for analogous Co and Ni complexes $[Co(tren)(pzac)](ClO_4)Cl$ (tren = tris-(2-aminoethyl)amine) and $[Ni(pzac)_2(H_2O)_2]$ [23,24]. The C9–O2 and C9–O3 distances in **1** are equal to 1.276 and 1.219 Å, respectively, which corresponds well to those found in $[Ni(pzac)_2(H_2O)_2]$ with distances 1.272 and 1.230 Å, respectively [24]. Similarly C8–O4 and C8–N6 distances are equal to 1.237 and 1.314 Å in **1** and 1.235 and 1.312 Å in the Ni complex, respectively. There are several known silver complexes both with 2,3-dicyanopyrazine and $pzac^-$ [25,26]. In $[Ag(pzac)]_n$ both oxygen atoms of a carboxyl group are involved in the coordination to the metal center, thus C–O distances are very similar and equal to 1.239 and 1.251 Å. The adjacent C=O and C–N distances in the amido group of $[Ag(pzac)]_n$ are 1.227 and 1.332 Å, respectively [26].

Table 2
Selected bond lengths (Å) and angles (°) in **1**.

Bond lengths		Bond angles	
Mo1–O1	1.6681(13)	C2–Mo1–O1	101.75(7)
Mo1–O2	2.1619(12)	C2–Mo1–O2	93.94(6)
Mo1–C1	2.176(2)	C2–Mo1–C1	89.61(7)
Mo1–C2	2.151(2)	C2–Mo1–C3	86.60(7)
Mo1–C3	2.187(2)	O1–Mo1–O2	164.30(6)
Mo1–N4	2.1689(16)	O1–Mo1–N4	91.97(7)
N1–C1	1.134(2)	O1–Mo1–C1	97.16(7)
N2–C2	1.136(2)	O1–Mo1–C2	101.75(7)
N3–C3	1.134(2)	O1–Mo1–C3	97.80(7)
N4–C4	1.348(2)	O2–Mo1–N4	72.33(6)
C4–C5	1.369(3)	O2–Mo1–C1	82.68(6)
C5–N5	1.337(2)	O2–Mo1–C3	83.13(6)
C6–N5	1.339(3)	N4–Mo1–C1	88.59(6)
C6–C7	1.397(2)	N4–Mo1–C3	91.65(6)
N4–C7	1.351(2)	C1–Mo1–C3	165.02(7)
C6–C8	1.517(3)	Mo1–C1–N1	178.18(19)
C7–C9	1.512(3)	Mo1–C2–N2	175.93(17)
O2–C9	1.276(2)	Mo1–C3–N3	178.17(19)
O3–C9	1.219(2)		
O4–C8	1.237(2)		
N6–C8	1.314(2)		

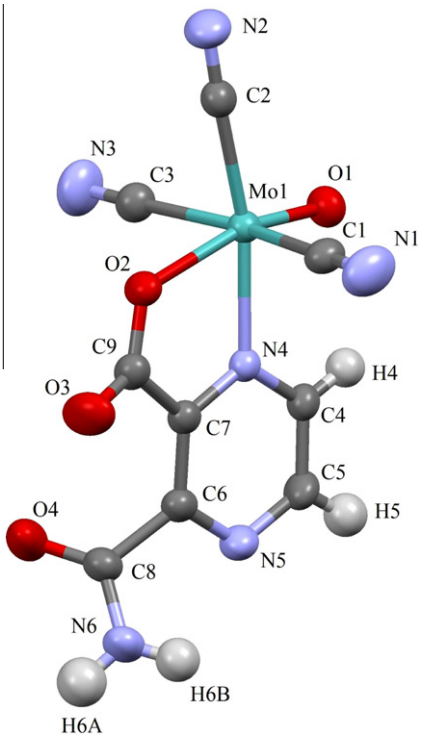

Fig. 1. Single-crystal X-ray structure of $[Mo(CN)_3O(pzac)]^{2-}$ showing the atom labeling scheme and 50% displacement ellipsoids.

The crystal packing is presented in Fig. 2. The cations and anions are mixed between each other and, contrary to many $[Mo(CN)_3O(LL)]^{n-}$ ion salts, no separated layers of anions can be isolated.

The water molecules and anions are involved in a complicated network of hydrogen bonds, as presented in Fig. 3. One water molecule O6, forms a strong hydrogen bond to the carbonyl oxygen O3 with a relatively short distance of 2.782 Å and to N6 with a distance of 3.130 Å. The second water molecule O5 forms hydrogen bonds with O1 (2.975 Å) and N2 (2.860 Å) from another anion, thus forming a bridge between two anions. Second type of inter-anion supramolecular bridge is formed by hydrogen bonds between amine and carbonyl groups. The N6–O4′ distance is equal to 2.949 Å. Similar hydrogen interactions between amine groups of adjacent anions were found in the silver salt with almost identical N–O distance (2.947 Å) [26].

The described network of hydrogen bonds generates circles involving four adjacent anions with the radius of 6.558 Å. Each circle is composed in such a way that planes formed by C(8)–N(6)–O(4′)–C(8′)–N(6′)–O(4) atoms are parallel to each other with the interplane distance of 5.524 Å. All anions are thus involved in a two-dimensional layer, there are no interactions between such separated layers. In the silver salt of $pzca^-$, no such interactions were observed [26]. This is a result of the PPh_4^+ cation presence, that makes the three dimensional network less rigid.

The anion structure of **2** is presented in Fig. 4, the estimated bond lengths and angles are given in Table 3.

The anion structure indicates that the nitrile group was converted into the corresponding iminonitrile, similarly as it was found in our previous paper for 2-pyrazinecarbonitrile [13]. The organic ligand is coordinated in a similar mode (with imine and pyridine nitrogen atoms coordinated to the Mo center) and the anion structure is typical as for the other $[Mo(CN)_3O(LL)]^{n-}$ anions. The

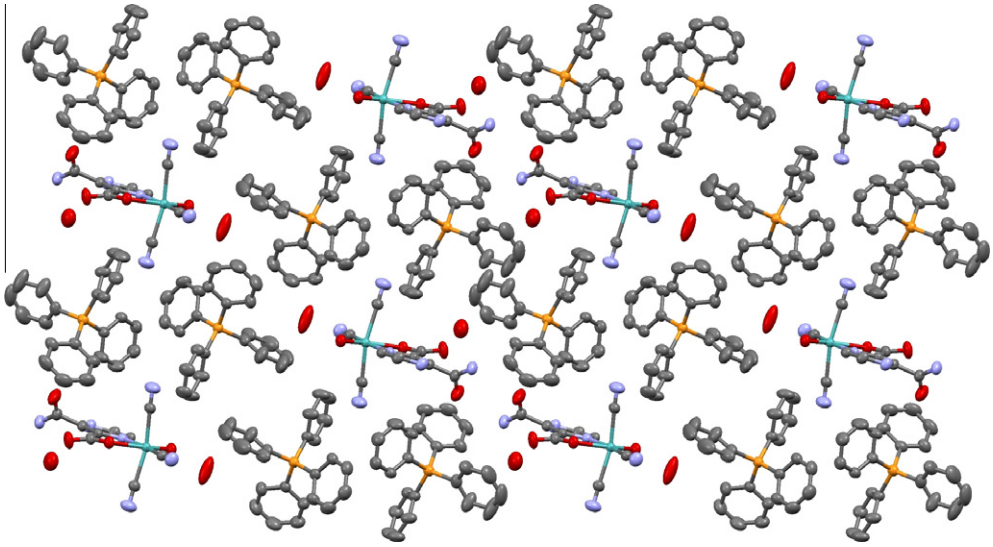

Fig. 2. Crystal packing in **1**.

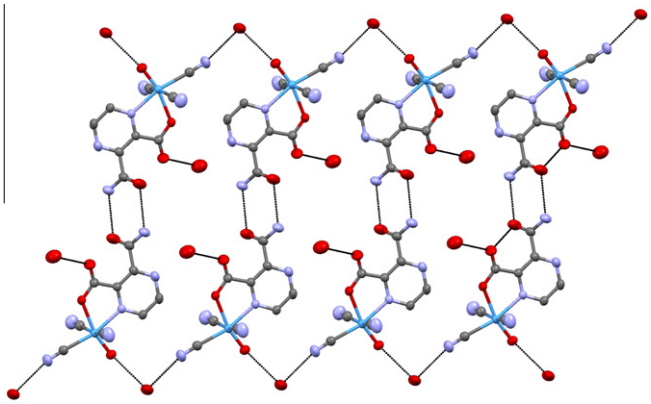

Fig. 3. The hydrogen bonds network in **1**. The cations and hydrogen atoms are omitted for clarity.

bond lengths and angles are very similar to that found in **1** but since its structure was determined with high R factors we do not compare in details the structure properties.

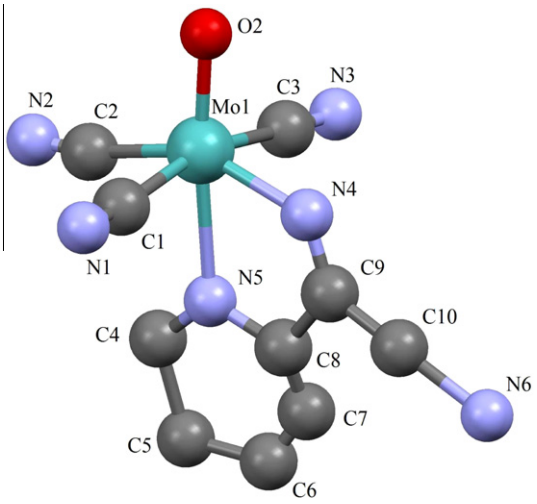

Fig. 4. Single-crystal X-ray structure of $[Mo(CN)_3O(pzac)]^{2-}$ showing the atom labeling scheme and 50% displacement ellipsoids.

Table 3
Selected bond lengths (Å) and angels (°) in **2**.

Bond lengths		Bond angles	
Mo–C3	2.1151	C3–Mo–O	97.22
Mo–O	1.8199	C3–Mo–C2	90.94
Mo–C2	1.9946	C3–Mo–N4	85.68
Mo–N4	1.9858	C3–Mo–C1	165.55
Mo–C1	2.1326	C3–Mo–N5	81.32
Mo–N5	2.3138	O–Mo–C2	105.06
C3–N3	1.1593	O–Mo–N4	105.31
C2–N2	0.9792	O–Mo–C1	96.64
N4–C9	1.2087	O–Mo–N5	173.36
C1–N1	1.1829	C2–Mo–N4	149.63
C9–C10	1.3971	C2–Mo–C1	89.39
C10–N6	1.6355		

3.2. IR spectra

Spectral data of **1** and **2**, presented in Figs. 5 and 6, are consistent with the proposed complex composition and with the X-ray structures. The $\nu_{Mo=O}$ band positions in **1** and **2** (959 and 927 cm^{-1}, respectively) are in the range typical for analogous $[Mo(CN)_3O(LL)]^{n-}$ complexes, where LL can be OO, NO or NN-donor ligands [20]. For **1** its position is the closest to that in complex with the picolinic acid (NO donating as in **1**) ligand (950 cm^{-1}) [21]. For complex **2**, low energy of the $\nu_{Mo=O}$ band suggests relatively strong bonding of pyridinecyanoimine. In the $[Mo(CN)_3O(pnccn)]^{2-}$ complex, with analogous 2-pyrazinecyanoimine ligand, the $\nu_{Mo=O}$ band is observed at 932 cm^{-1} [13]. Such a low position of this band in **2** additionally supports the cyanoimine formation.

In the region characteristic for CN stretching vibrations (2100–2200 cm^{-1}) bands attributed to cyano ligands and nitrile group can be observed. In salt **1** only bands of this first origin are observed as all ligand nitrile groups were hydrolyzed to carboxylic or imine groups. For compound **1** ν_{CN} bands are located at 2101 and 2113 cm^{-1}. For the closest analogue, complex with NO donating picolinic acid, bands are observed at 2097 and 2110 cm^{-1} [19]. For compound **2** ν_{CN} bands are observed at 2109 and 2092 cm^{-1}, in the range typical for NN donating ligands. Additionally a third band at 2166 cm^{-1} is observed for **2**. This band can be assigned to the stretching vibrations of a nitrile substituent in the pynccn$^-$ ligand; the position of this band clearly indicates that the nitrile group is not coordinated to the metal.

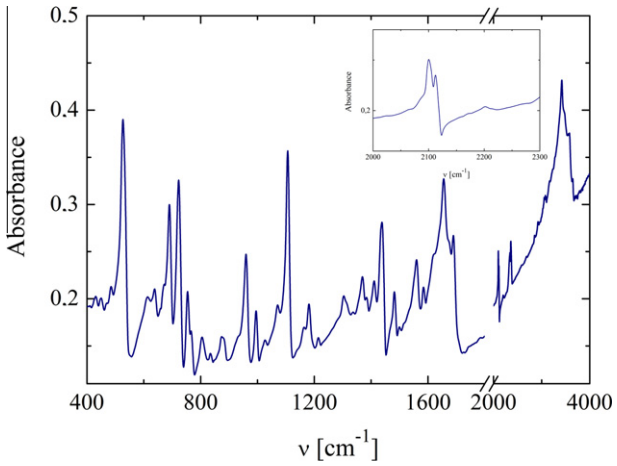

Fig. 5. IR spectrum of **1** in KBr.

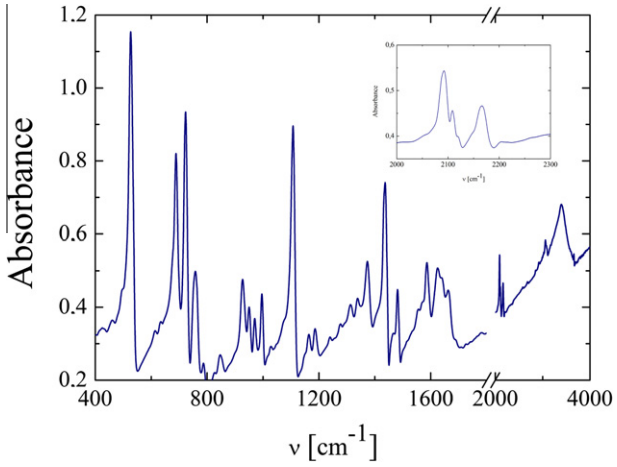

Fig. 6. IR spectrum of **2** in KBr. The upper right corner represents the 2000–2300 cm^{-1} part of the spectrum.

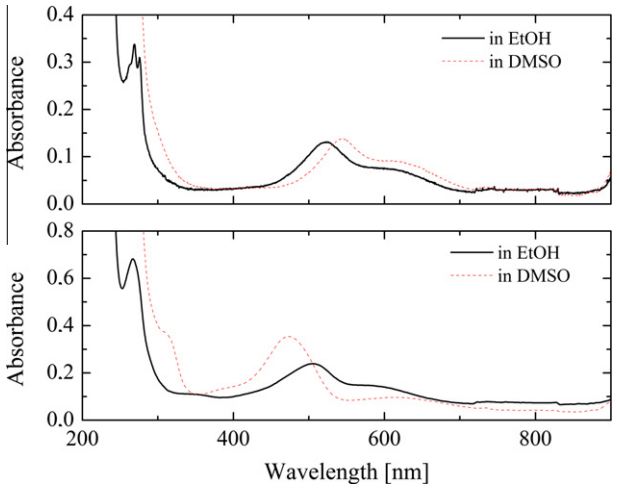

Fig. 7. UV–Vis spectra of **1** (upper) and **2** in DMSO and EtOH.

In the C=O stretching vibration region, only one strong band at 1690 cm^{-1} is observed for **1**. The disappearance of the band at 1733 cm^{-1} characteristic for Hpzac (attributed to the carboxylic oxygen) and a small shift of the C=O band of an amide group (from 1677 cm^{-1} in Hpzac to 1690 cm^{-1} in **1**) is consistent with the structure and indicates the presence of a pendant carbonyl oxygen of the amide group [27]. The significant change of a position of ν(C=O) band in the amide group (from 1677 to 1690 cm^{-1}) can be a result of both coordination of $pzac^-$ ligand to the molybdenum center (leading to charge distribution changes on the ligand) and formation of strong intermolecular hydrogen bonds with NH_2 group of an adjacent anion (see Fig. 3).

In the other regions, the most characteristic bands typical for PPh_4^+ cation (at 1100 cm^{-1} and at 997 cm^{-1}) can be also observed for both compounds.

3.3. UV–Vis spectra

The UV–Vis absorbance spectra of **1** and **2** are presented in Fig. 7. In the UV part, the spectra are dominated by the bands of PPh_4^+ cations while the visible parts are dominated by the intense MLCT (metal-to-ligand charge-transfer) transitions overlapping with *d–d* transitions at the low energy end of the spectra. For both compounds **1** and **2** the solvatochromism of the MLCT transitions is observed, as presented in Fig. 7. The most intense MLCT bands show a batochromic shift from 522 (in EtOH) to 544 nm (in DMSO) for **1** and from 472 (in EtOH) to 482 nm (in DMSO) for **2**. The analogous spectral behavior with the solvatochromism of MLCT bands has also been found for all other Mo(IV) complexes $[Mo(CN)_3O(LL)]^{n-}$ [20].

The reflectance spectra of **1** and **2** are presented in Fig. 8. The lowest energy bands are observed at 505 nm for **1** and at 636 nm for **2**. These bands are almost at the same position as in solution and are solvatochromic (Fig. 7). Moreover, they are relatively intense, compared to the UV bands (see Fig. 7) what indicates their CT (charge-transfer) character. For $[Mo(CN)_3O(LL)]^{n-}$ complexes the lowest energy bands in reflectance spectra were attributed to *d–d* transitions but this is not the case for the studied salts. The CT bands of MLCT origin (metal-to-ligand CT) are typically observed for all $[Mo(CN)_3O(LL)]^{n-}$ complexes in the visible part of the spectra. However, it has been found that the lowest energy band of *d–d* character overlaps with the closest CT band [20]. In salts **1** and **2** the observed solvatochromism of the lowest energy bands indicates mostly their CT character obscuring less intense *d–d* bands.

3.4. Cyclic voltammetry measurements

The cyclic voltammetry measurements carried out in DMSO are presented in Figs. 9 and 10 for **1** and **2**, respectively. The measurements indicate that salt **1** undergoes irreversible oxidation at 0.57 V. However, when the measurement range is limited to the oxidation peak, it can be seen that oxidation potential is merely dependent on the scan speed (in the 20–1000 mV/s range), what is typical rather for a quasi-reversible than an irreversible oxidation. On the other hand, no reduction wave is observed at all scan speeds. Such a behavior is indicative for an irreversibility caused by the chemical reaction following oxidation of the complex and not by the complex itself.

The cyclic voltammogram of **2** is presented in Fig. 12. The salt undergoes reversible oxidation/reduction at $E^0_{1/2}$ = 0.300 V with the peak separation of 0.12 V at 100 mV/s scan speed. The observed redox processes both for **1** and **2** can be attributed to a Mo(IV/V) redox couple. For **1** the reduction wave observed at −1.17 V can be attributed to a ligand-centered process, probably involving the amide group. For **2** such a reduction wave is not observed since the amide group is not present in this compound.

3.5. The reaction of Mo(IV) with nitriles studied in at different pH

To study the formation of **1** and **2** in the reaction of $K_3Na[Mo(CN)_4O_2]\cdot 6H_2O$ with nitriles, the spectroscopic studies in

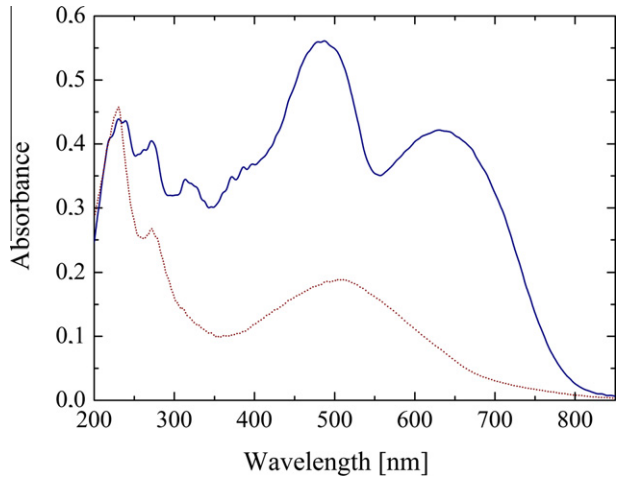

Fig. 8. UV–Vis reflectance spectra of **1** (dotted line) and **2** (solid line) in $BaSO_4$ after Kubelka–Munk transformation.

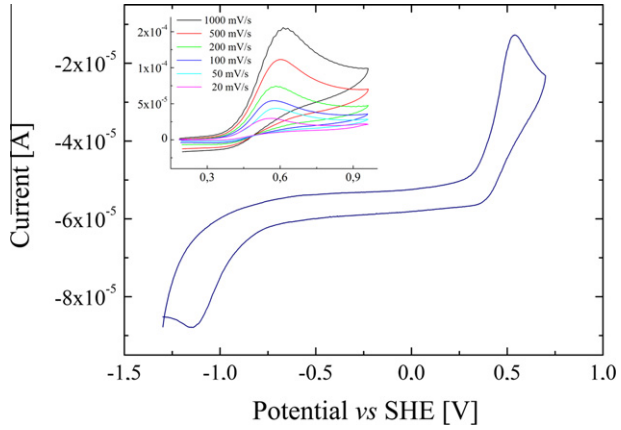

Fig. 9. Cyclic voltammogram of **1** in 0.1 M Bu_4NPF_6 DMSO as electrolyte. In the upper left corner voltammograms recorded at different scan speeds are shown.

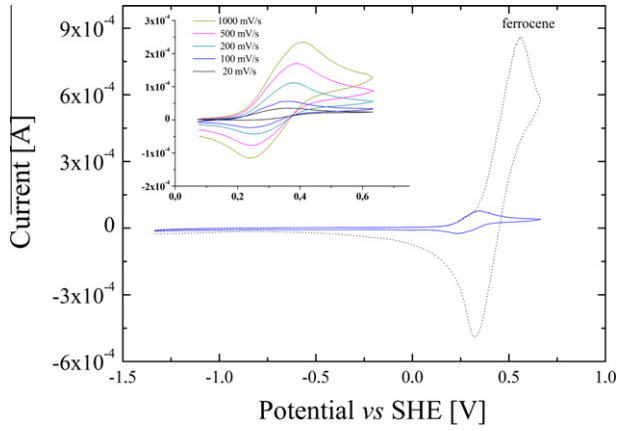

Fig. 10. Cyclic voltammogram of **2** in 0.1 M Bu_4NPF_6 DMSO as electrolyte. The dotted line represents the voltammogram with ferrocene used as an internal potential standard. In the upper left corner voltammograms recorded at different scan speeds are shown.

the UV–Vis range were performed in H_2O–EtOH (2:1 v/v) mixture at different pH values (8.5, 9.5, 10.5 and 11.5). These pH values were purposely selected to obtain various ratios of two protonation forms of the Mo(IV) complex; at pH = 8.5 and 9.5 the $[Mo(CN)_4O(H_2O)]^{2-}$ ion prevails ($pK = 9.70$) and at pH = 10.5 and above $[Mo(CN)_4O(OH)]^{3-}$ is in excess [28,29].

The spectral changes observed during the reaction of Mo(IV) with 2,3-dicyanopyrazine at different pH are presented in Figs. 11 and 12.

The UV part shows bands associated with 2,3-dicyanopyrazine, this is a result of not only their much more intensity but also higher concentration of the ligand compared to the complex (25:1 molar ratio). In general, the character of spectral changes seems to be independent on pH. With reaction time, the band at 228 nm decreases, the band at 276 nm remains almost unaltered whereas the increase of absorption at 300 nm is observed. Not well resolved isosbestic point at 218 nm is observed at all pH studied, whereas another isosbestic point, at 258 nm, is observed at all pH values except pH = 8.5. After 2 h the reaction seems to be completed. The complicated spectral changes are connected with the nitrile hydrolysis and it seems that 2,3-dicyanopyrazine, after 2 h (at pH = 9.5 and above) is totally converted into a final product. Since the ligand to complex ratio is 25:1, the conversion of this ligand has to be a catalytical process. In Fig. 13 it can also be seen that the rate of the nitrile hydrolysis depends strongly on pH. At pH = 8.5 the slowest spectral changes are observed, whereas at pH > 8.5 the reaction is accelerated. This is a typical behavior for a basic nitrile hydrolysis.

In the visible part of the spectra (Fig. 12) the changes are much more complicated. In this spectral region only the bands of molybdenum complexes can be observed, as the nitrile and the products of its hydrolysis do not absorb in this region. Since the Mo(IV) complexes $[Mo(CN)_4OL]^{n-}$ (where L is a monodentate ligand) exhibit only *d*–*d* transitions (above 500 nm) of low intensity [20], bands of such complexes cannot be clearly observed in Fig. 12 due to the low concentration of the initial complex. However, complexes of $[Mo(CN)_3O(LL)]^{n-}$ type have intense CT bands in the visible region and their formation can be easily studied under reaction conditions. What is more important, such complexes can be formed at pH < 9.7, where the labile aqua form of the Mo(IV) complex is dominant. This is an explanation of spectral changes presented in Fig. 12. At pH = 8.5 formation of the final complex **1** can be easily seen, whereas with increasing pH smaller amount of the complex is formed. The observed spectral changes in Fig. 12 are much more complicated since the hydrolysis of 2,3-dicyanopyrazine leads to several products that can bind to the molybdenum center in a bidentate mode. For example, the band at *ca.* 420 nm, observed at the beginning of the reaction, can be attributed to the molybdenum complex with 2-monocarbox-3-cyanopyrazinemonoamine.

The considerably different pathway is observed for 2-pyridinecarbonitrile, as illustrated in Fig. 13 in the UV part of the electronic spectra. The spectral changes indicate very little ligand conversion to the final product. This can be interpreted as a different way of ligand transformation. If the hydroxyl group could attack the nitrile group, activated by its coordination to the molybdenum center, the conversion into amide should occur catalytically and the total conversion of the nitrile into a corresponding amide and/or 2-pyridinecarboxylic acid should be observed, similarly as it was for 2-dicyanopyrazine. Contrary to this, however, the amount of the ligand transformed is very small and it correlates with the amount of the $[Mo(CN)_3O(pynccn)]^{2-}$ formed. Moreover, the amount of the resulting $[Mo(CN)_3O(pynccn)]^{2-}$ remains very low even at pH = 8.5 and decreases with the pH increase. The first step of the reaction is the coordination of 2-pyridinecarbonitrile to the molybdenum center. The ligand is coordinated in a monodentate way via the nitrogen atom. It can be either pyridine or nitrile nitrogen. This nitrogen atom must occupy the initial position of the aqua ligand since the aqua ligand is the labile one. This coordination does not seem to initiate the ligand hydrolysis since no corresponding spectral changes are observed. In the next reaction step, a cyano ligand, released from the complex, attacks the nitrile group

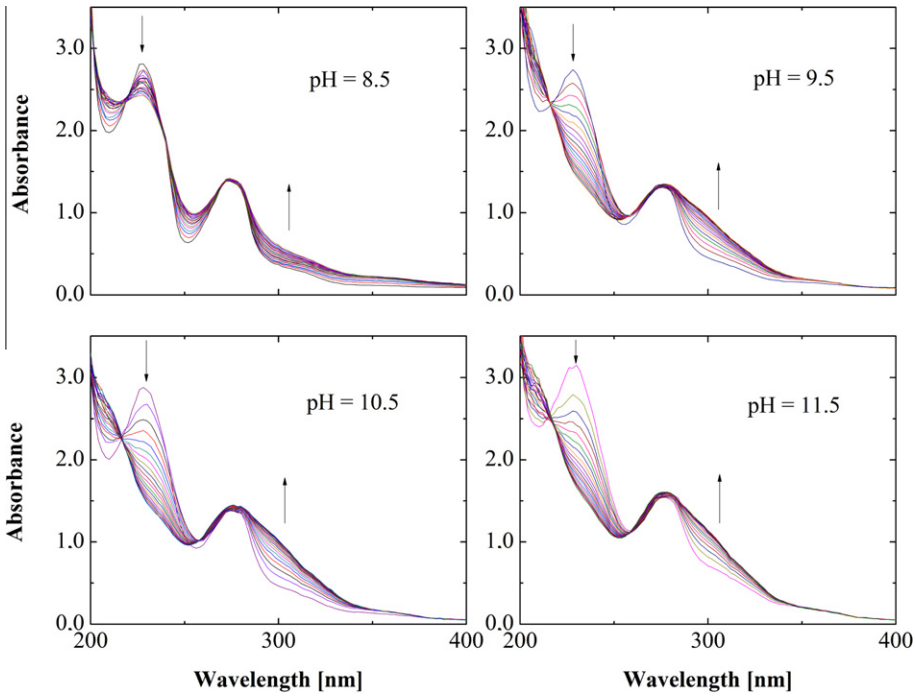

Fig. 11. UV electronic spectra during the reaction of $K_3Na[Mo(CN)_4O_2]\cdot 6H_2O$ with 2,3-dicyanopyrazine at different pH. $T = 313$ K, [Mo] = $1.05 \cdot 10^{-4}$ M, [2,3-dicyanopyrazine] = $2.6 \cdot 10^{-3}$ M, $d = 1$ cm, H_2O–EtOH (2: 1 v/v). Spectra measured every 350 s. The arrows indicate the direction of the changes.

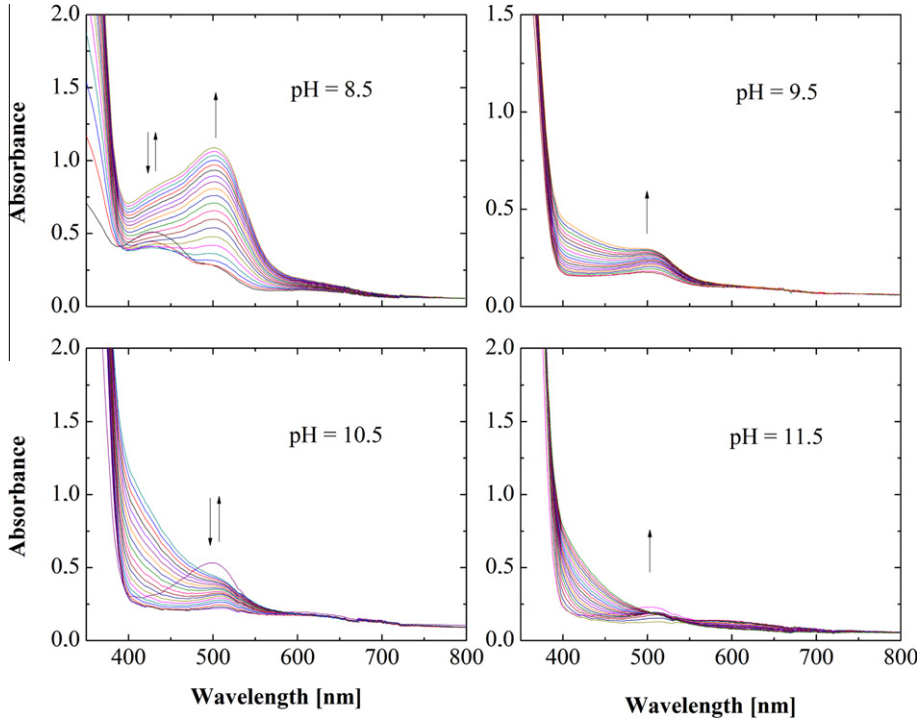

Fig. 12. Visible electronic spectra during the reaction of $K_3Na[Mo(CN)_4O_2]\cdot 6H_2O$ with 2,3-dicyanopyrazine at different pH. $T = 313$ K, [Mo] = $4.0 \cdot 10^{-3}$ M, [2,3-dicyanopyrazine] = 0.1 M, $d = 1$ cm, H_2O–EtOH (2:1 v/v). Spectra measured every 350 s. The arrows indicate the direction of the changes.

with the formation of pynccn$^-$. Since the amount of released cyano ligand is equal to the amount of resulting **2**, it explains the lack of the catalytical effect of the metal on the ligand transformation and the small conversion of the nitrile. It seems that the reactive form is that with a pyridine nitrogen coordinated to the molybdenum center. This is not a favorable coordination since the nitrile group has to be located between cyano ligands, otherwise there would be too big steric hindrance. However, in this case the cyano ligand is very close to the nitrile group and the nitrilation of the nitrile is easier. Such a mechanism is also supported by the X-ray crystal structure of the cyanolysis product, where the pyridine nitrogen is in the *trans* position to the oxo ligand. Thus the mechanism seems to be very similar to that suggested for the nitrilation of 2-pyrazinenitrile [13].

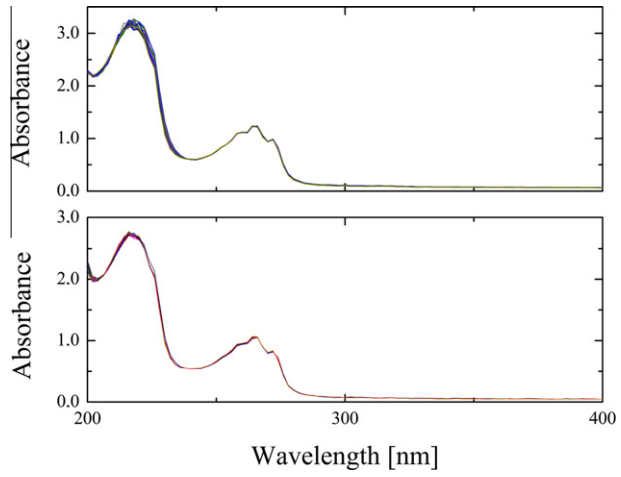

Fig. 13. UV electronic spectra during the reaction of $K_3Na[Mo(CN)_4O_2]\cdot 6H_2O$ with 2-pyridinecarbonitrile at pH = 8.5 (up) and pH = 10.5 (down). T = 313 K, [Mo] = $1.05 \cdot 10^{-4}$ M, [2-pyridinecarbonitrile] = $2.6 \cdot 10^{-3}$ M, d = 1 cm, H_2O–EtOH (2: 1 v/v). Spectra measured every 350 s.

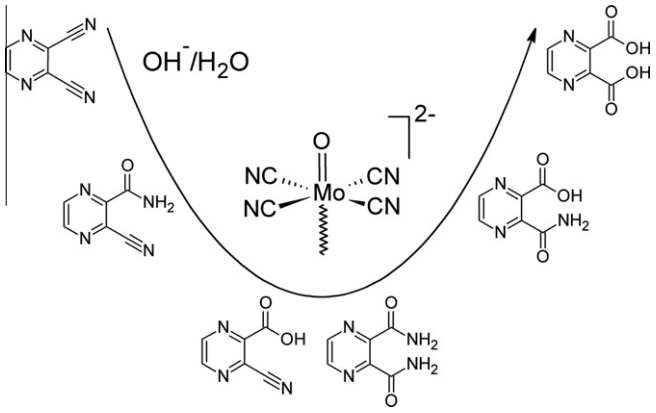

Scheme 1. Hydrolysis of 2,3-pyrazinecarbodinitrile in the presence of cyanooxomolybdates(IV).

4. Conclusion

The reaction of two different nitriles, 2,3-dicyanopyrazine and 2-pyridinecarbonitrile revealed two possible pathways of a nucleophilic attack on the nitrile group; it is either attacked by OH^- or CN^- ion. By means of a Mo(IV) complex it has been possible to trap the products of ligands transformations formed on different reaction pathways. In the case of 2,3-dicyanopyrazine, the complex with 2,3-pyrazinedicarboxylatomonoamide ligand has been isolated, whereas in the case of 2-cyanopyridine the complex with 2-pyridinecyanoimine has been obtained. The simplified scheme of the hydrolysis of 2,3-dicyanopyrazine is presented in Scheme 1.

It seems that similarly as postulated in our previous paper, the coordination of Mo(IV) to aromatic nitrogen is responsible for the observed nitrile reactivity [13]. In the case of 2,3-pyrazinecarbonitrile the attack of hydroxyl group on a nitrile in the *meta* position to pyrazine nitrogen (coordinated to Mo) yields the amide whereas in the case of 2-pyridinecarbonitrile the lack of such possibility results in slow attack of cyanide on a nitrile group. The spectral measurements indicate non-catalytical cyanolysis of a nitrile followed by the formation of **2**, as well as catalytical hydrolysis of 2,3-pyrazinecarbonitrile, with the formation of **1** limited by the amount of initial molybdenum complex.

Appendix A. Supplementary data

CCDC 873340 contains the supplementary crystallographic data for **1**. These data can be obtained free of charge *via* http://www.ccdc.cam.ac.uk/conts/retrieving.html, or from the Cambridge Crystallographic Data Centre, 12 Union Road, Cambridge CB2 1EZ, UK; fax: (+44) 1223-336-033; or e-mail: deposit@ccdc.cam.ac.uk. Supplementary data associated with this article can be found, in the online version, at http://dx.doi.org/10.1016/j.poly.2012.07.006.

References

[1] (a) B. Gao, Q. Zhou, Y. Geng, Y. Cheng, D. Ma, Z. Xie, L. Wang, F. Wang, Mater. Chem. Phys. 99 (2006) 247;
(b) S. Chew, P. Wang, Z. Hong, H.K. Kwong, J. Tang, S. Sun, C.S. Lee, S.-T. Lee, J. Lumin. 124 (2007) 221.
[2] R. Cristiano, E. Westphal, I.H. Bechtold, A.J. Bortoluzzi, H. Gallardo, Tetrahedron 63 (2007) 2851.
[3] (a) P. Albores, E. Rentschler, Angew. Chem., Int. Ed. 48 (2009) 9366;
(b) M.M. Turnbull, G. Pon, R.D. Willett, Polyhedron 10 (1991) 1835;
(c) T. Otieno, S.J. Rettig, R.C. Thompson, J. Trotter, Can. J. Chem. 68 (1990) 1901;
(d) O.-S. Jung, C.G. Pierpont, J. Am. Chem. Soc. 116 (1994) 2229;
(e) D. Venkataraman, S. Lee, J.S. Moore, P. Zhang, K.A. Hirsch, G.B. Gardner, A.C. Covey, C.L. Prentice, Chem. Mater. 8 (1996) 2030;
(f) L. Carlucci, G. Ciani, D.M. Proserpio, A. Sironi, Angew. Chem., Int. Ed. Engl. 34 (1995) 1895;
(g) L. Carlucci, G. Ciani, D.M. Proserpio, A. Sironi, Inorg. Chem. 34 (1995) 5698;
(h) T. Soma, H. Yuge, T. Iwamoto, Angew. Chem., Int. Ed. Engl. 33 (1994) 1665;
(i) L. Carlucci, G. Ciani, D.M. Proserpio, A. Sironi, J. Am. Chem. Soc. 117 (1995) 4562;
(j) T. Otieno, S.J. Rettig, R.C. Thompson, J. Trotter, Inorg. Chem. 32 (1993) 1607;
(k) L.R. MacGillivray, S. Subramanian, M.J. Zaworotko, J. Chem. Soc., Chem. Commun. (1994) 1325;
(l) M.A. Withersby, A.J. Blake, N.R. Champness, P. Hubberstey, W.-S. Li, M. Schroder, Angew. Chem., Int. Ed. Engl. 36 (1997) 2327;
(m) L. Carlucci, G. Ciani, D.M. Proserpio, A. Sironi, Inorg. Chem. 37 (1998) 5941;
(n) M.J. Hannon, C.L. Painting, W. Errington, J. Chem. Soc., Chem. Commun. (1997) 1805;
(o) Y. Suenaga, T. Kuroda-Sowa, M. Munakata, M. Maekawa, Polyhedron 18 (1999) 191.
[4] (a) J.Y. Jaung, M. Matsuoka, K. Fukunishi, Dyes Pigments 40 (1998) 11;
(b) B.H. Lee, J.Y. Jaung, Dyes Pigments 59 (2003) 125.
[5] C. Sablayrolles, G.H. Cros, J.C. Milhavet, E. Rechenq, J.P. Chapat, M. Boucard, J.J. Serrano, J.H. McNeill, J. Med. Chem. 27 (1984) 206.
[6] A. Trejo, H. Arzeno, M. Browner, S. Chanda, S. Cheng, D.D. Comer, S.A. Dalrymple, P. Dunten, J. Lafargue, B. Lovejoy, J. Freire-Moar, J. Lim, J. Mcintosh, J. Miller, E. Papp, D. Reuter, R. Roberts, F. Sanpablo, J. Saunders, K. Song, A. Villasenor, S.D. Warren, M. Welch, P. Weller, P.E. Whiteley, L. Zeng, D.M. Goldstein, J. Med. Chem. 46 (2003) 4702.
[7] G.G. Dubinina, M.O. Platonov, S.M. Golovach, P.O. Borysko, A.O. Tolmachov, Y.M. Volovenko, Eur. J. Med. Chem. 41 (2006) 727.
[8] E.H. Moekved, Chem. Heterocycl. Compd. 43 (2007) 1197.
[9] (a) S. Makhseed, J. Samuel, F. Ibrahim, Tetrahedron 64 (2008) 8871;
(b) P. Zemcik, M. Miletin, V. Novakova, K. Kopecky, Z. Dvorakova, Dyes Pigments 81 (2009) 35;
(c) D. Hou, M. Matsuoka, Dyes Pigments 22 (1993) 1117;
(d) R.Z.U. Kobak, E.S. Öztürk, A. Koca, A. Gül, Dyes Pigments 86 (2010) 115.
[10] (a) B.H. Lee, J.Y. Jaung, S.C. Jang, S.C. Yi, Dyes Pigments 65 (2005) 159;
(b) J.-Y. Jaung, Dyes Pigments 72 (2007) 315. and references therein.
[11] (a) A.J.L. Pombeiro, V.Y. Kukushkin, in: J.A. McCleverty, T.J. Meyer (Eds.), Comprehensive Coordination Chemistry II, vol. 1, Elsevier, Oxford, UK, 2004, p. 639 (Chapter 1.34);
(b) V.Y. Kukushkin, A.J.L. Pombeiro, Chem. Rev. 102 (2002) 1771;
(c) V.Y. Kukushkin, A.J.L. Pombeiro, Inorg. Chim. Acta 358 (2005) 1.
[12] D. Matoga, J. Szklarzewicz, K. Lewiński, Polyhedron 27 (2008) 2643.
[13] D. Matoga, J. Szklarzewicz, K. Lewiński, Polyhedron 29 (2010) 94.
[14] J. Szklarzewicz, A. Samotus, D. Matoga, Ann. Pol. Chem. Soc. (2001) 273. and references therein.
[15] J. Szklarzewicz, A. Gruszewska, Trans. Met. Chem. 30 (2005) 27.
[16] A. Samotus, M. Dudek, A. Kanas, J. Inorg. Nucl. Chem. 37 (1975) 943.
[17] R.G. Bates, Determination of pH – Theory and Practice, Wiley & Sons, New York, 1965.
[18] A. Altomare, G. Cascarano, G. Giasovazzo, A. Guagliardi, M.C. Burla, G. Polidori, M. Camalli, J. Appl. Crystallogr. 27 (1994) 435.
[19] G.M. Sheldrick, Acta Crystallogr., Sect. A 64 (2008) 112.
[20] A. Samotus, J. Szklarzewicz, D. Matoga, Bull. Pol. Acad. Sci., Chem. 50 (2002) 145.
[21] J. Szklarzewicz, A. Makuła, D. Matoga, J. Fawcett, Inorg. Chim. Acta 358 (2005) 1749.
[22] B.J. Coe, S.J. Glenwright, Coord. Chem. Rev. 203 (2000) 5.

[23] U. Mukhopadhyay, R. Galian, I. Bernal, Inorg. Chim. Acta 362 (2009) 4237.
[24] R.H. Heyn, P.D.C. Dietzel, J. Coord. Chem. 60 (2007) 431.
[25] Y. Suenaga, T. Kamiya, T. Kuroda-Sowa, M. Maekawa, M. Munakata, Inorg. Chim. Acta 308 (2000) 17.
[26] A.A. Massoud, V. Langer, M.A.M. Abu-Youssef, L. Ohrström, Acta Crystallogr., Sect. C 67 (2011) m1.
[27] SDBS, Spectral Database for Organic Compounds. Available from: <http://riodb01.ibase.aist.go.jp/sdbs/cgi-bin/direct_frame_top.cgi>.
[28] E. Hejmo, A. Kanas, A. Samotus, Bull. Acad. Polon. Sci. Ser. Sci. Chim. 21 (1973) 311.
[29] A. Kanas, M. Dudek, A. Samotus, Bull. Acad. Polon. Sci. Ser. Sci. Chim. 24 (1976) 43.